Cell-cycle-regulated association of RAD50/MRE11/NBS1 with TRF2 and human telomeres

Xu-Dong Zhu[1], Bernhard Küster[2], Matthias Mann[2], John H.J. Petrini[3] & Titia de Lange[1,5]

Telomeres allow cells to distinguish natural chromosome ends from damaged DNA and protect the ends from degradation and fusion. In human cells, telomere protection depends on the TTAGGG repeat binding factor, TRF2 (refs 1–4), which has been proposed to remodel telomeres into large duplex loops[5] (t-loops). Here we show by nanoelectrospray tandem mass spectrometry that RAD50 protein is present in TRF2 immunocomplexes. Protein blotting showed that a small fraction of RAD50, MRE11 and the third component of the MRE11 double-strand break (DSB) repair complex, the Nijmegen breakage syndrome protein (NBS1), is associated with TRF2. Indirect immunofluorescence demonstrated the presence of RAD50 and MRE11 at interphase telomeres. NBS1 was associated with TRF2 and telomeres in S phase, but not in G1 or G2. Although the MRE11 complex accumulated in irradiation-induced foci (IRIFs) in response to γ-irradiation, TRF2 did not relocate to IRIFs and irradiation did not affect the association of TRF2 with the MRE11 complex, arguing against a role for TRF2 in DSB repair. Instead, we propose that the MRE11 complex functions at telomeres, possibly by modulating t-loop formation.

We found that TRF2 complex isolated by immunoprecipitation from heparin-sepharose fractionated HeLa nuclear extract contains polypeptides migrating at 150 kD, 70 kD and 60 kD (Fig. 1*a*). Because these bands were consistently observed in TRF2 immunoprecipitates and not in control experiments with pre-immune serum, we characterized their identity by nanoelectrospray tandem mass spectrometry of tryptic peptides[6]. The sequence of peptides from the 60-kD band is identical to that of RAP1, the human orthologue of budding yeast Rap1p and recently identified as a TRF2-interacting factor in a yeast two-hybrid screen[7]. As expected, the 70-kD doublet contained TRF2. Human RAP1 and TRF2 were recovered at apparent 1:1 stoichiometry (Fig. 1*a*).

The sequence of 9 peptides from the 150-kD band identified RAD50 (Fig. 1*b*). RAD50 is stably associated with MRE11 and NBS1 (refs 8,9) in a complex that functions in the response to DSBs in both yeast and mammals[10]. The human MRE11 complex functions in DNA-damage detection and induction of an S-phase checkpoint[11,12], whereas studies in *Saccharomyces cerevisiae* indicate a key function in recombinational DNA repair and telomere maintenance[13–17]. Given the conservation of MRE11 and RAD50, it is probable that the mammalian MRE11 complex also functions in recombinational DNA repair. In agreement with this hypothesis is the observation that the mouse gene *Rad50* is essential[18,19].

TRF2 immunoprecipitates collected with two unrelated TRF2 sera (#508 and #647) contained RAD50, MRE11, NBS1 and RAP1 (Fig. 1*c*). Other telomeric proteins, including TRF1 and tankyrase, were not recovered with TRF2. Immunoprecipitation of MRE11 or NBS1 brought down TRF2 (Fig. 1*d*), confirming the association of the MRE11 complex with TRF2. The MRE11 complex was also found in TRF2 immunoprecipitates from primary human fibroblasts (Fig. 1*e*). We estimate that the fraction of the MRE11 complex associated with TRF2 is relatively small (1–5% of HeLa RAD50 was recovered with TRF2; data not

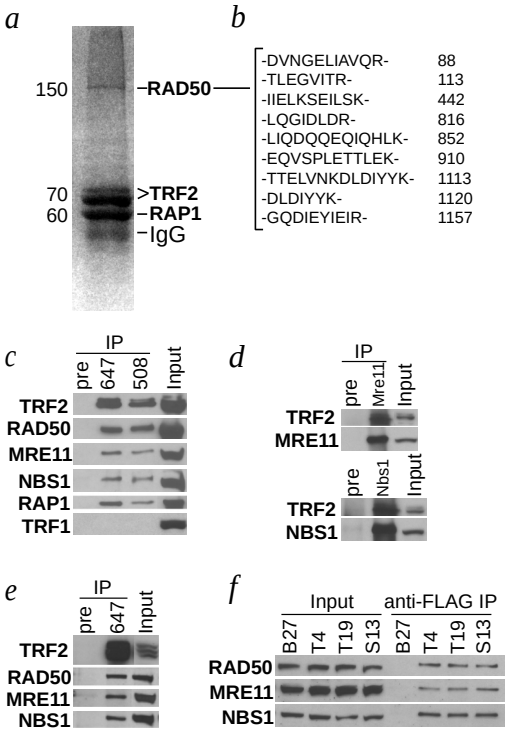

Fig. 1 Association of TRF2 with the MRE11 complex. ***a***, Identification of TRF2 associated proteins. Four bands that were consistently observed are indicated. ***b***, Identification of RAD50 by nanoelectrospray tandem mass spectrometry. Sequencing of nine tryptic peptides unambiguously identified the presence of human RAD50 in the 150-kD band. The position of the first amino acid of each peptide is given. ***c***, Co-immunoprecipitation of RAD50, MRE11 and NBS1 with TRF2. We carried out immunoprecipitations of HeLa nuclear extract using either pre-immune serum or anti-TRF2 antibodies (Ab#647 or Ab#508). We performed western-blot analysis with rabbit anti-RAD50, anti-MRE11 and anti-NBS1, anti-TRF2 (#647), anti-RAP1 (#765) and mouse anti-TRF1 sera (#3; S. Smith and T.d.L., unpublished data). ***d***, Co-immunoprecipitation of TRF2 with MRE11 and NBS1. We performed immunoprecipitations of HeLa nuclear extract using pre-immune serum, anti-MRE11 or anti-NBS1 antibodies. We performed western-blot analysis with rabbit anti-TRF2 (#647), anti-MRE11 and anti-NBS1. ***e***, Co-immunoprecipitation of the MRE11 complex with TRF2 from IMR90 cell extract. We carried out immunoprecipitations as described in (*c*), except we used whole-cell extract from young IMR90 cells. ***f***, DNA-binding activity of TRF2 is not required for association with the MRE11 complex. We carried out immunoprecipitations using antibody M2 and whole-cell extracts from HTC75-derived cell lines[3] induced to express FLAG-tagged TRF2$^{\Delta B \Delta M}$ (T4 and T19), FLAG-tagged TRF2$^{\Delta B}$ (S13) or no exogenous protein (B27). We performed western-blot analysis on the M2 immunocomplexes with rabbit anti-RAD50, anti-MRE1 and anti-NBS1. IP-M2, M2-immunoprecipitates.

[1]*The Rockefeller University, New York, New York, USA.* [2]*Protein Interaction Laboratory, University of Southern Denmark, Odense, Denmark.* [3]*Laboratory of Genetics, University of Wisconsin Medical School, Madison, Wisconsin, USA. Correspondence should be addressed to T.d.L. (e-mail: delange@rockvax.rockefeller.edu).*

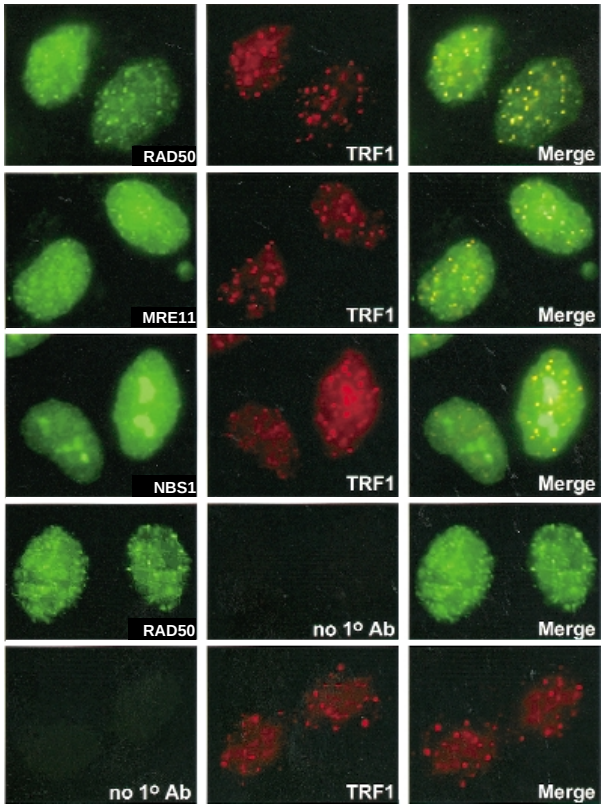

Fig. 2 Presence of RAD50, MRE11 and NBS1 at telomeres. ***a***, Co-localization of RAD50/MRE11/NBS1 with TRF1 at HeLa telomeres. We permeabilized interphase HeLa1.2.11 cells and stained with mouse anti-TRF1 antibody (TRITC) in conjunction with relevant rabbit anti-RAD50, anti-MRE11 and anti-NBS1 antibodies (FITC) as indicated. As a control for bleed-through of the FITC signal into the TRITC channel and vice versa, we stained detergent-extracted and fixed cell nuclei with either rabbit anti-RAD50 antibody alone (FITC) or mouse anti-TRF1 antibody alone (TRITC) and processed with both secondary antibodies. ***b***, Co-localization of RAD50/MRE11/NBS1 proteins with TRF1 in the ALT cell line WI38VA13/2RA. We extracted interphase cells with detergent and stained with the indicated antibodies as described above.

shown) and, in reciprocal fashion, only a minor fraction of TRF2 seemed to be associated with RAD50 (Fig. 1*a*). Other abundant nuclear proteins did not interact with TRF2 (GCN5 and XPA, data not shown), indicating that the association of TRF2 with the MRE11 complex was not simply due to its abundance.

We addressed the possibility that the association of TRF2 with RAD50/MRE11/NBS1 was mediated by DNA tethering in two cell lines (T4 and T19) that express TRF2$^{\Delta B\Delta M}$, a FLAG-tagged TRF2 deletion mutant lacking the DNA-binding domain[3]. Cell line S13, expressing a FLAG-tagged, DNA-binding competent version of TRF2 (TRF2$^{\Delta B}$; ref. 3), was characterized in parallel. The MRE11 complex was present in FLAG immunoprecipitates from S13, T4 and T19, but not in the B27-negative (empty vector) control (Fig. 1*f*), showing that recovery of MRE11 in TRF2 immunocomplex was not dependent on the DNA-binding activity of TRF2. Moreover, high salt conditions (500 mM KCl), which dissociated most of the TRF2 from telomeric DNA, did not disrupt the interaction of TRF2 with the MRE11 complex, nor did the MRE11 complex appear in TRF1 immunoprecipitates (data not shown). These data support an interaction between the MRE11 complex and TRF2, and argue against DNA tethering as the basis for their co-immunoprecipitation.

To examine the presence of RAD50/MRE11/NBS1 at telomeres, we used dual indirect immunofluorescence (IF) with TRF1, that is a specific marker for interphase telomeres[20,21]. Because the MRE11 complex shows a dispersed nuclear signal[9,11,12] that could mask its presence at telomeres, we performed IF studies after extraction of nucleoplasmic proteins with detergent. This treatment did not affect TRF1, TRF2 or RAP1 (data not shown). Unlike the bright overall staining of unextracted cells[22] (Fig. 4*a*), RAD50 antibody showed a punctate pattern in detergent-extracted interphase nuclei (Fig. 2*a*), suggesting that a small fraction of RAD50 located to specific subnuclear sites. This pattern was distinct from the radiation-induced foci, which are larger and less homogeneous in size[9,22] (Fig. 4*a*). Many of the sites of RAD50 staining were found to co-localize with TRF1, although non-telomeric RAD50 was also observed. We could not establish whether all telomeres contained RAD50. MRE11 generally showed a more homogenous nuclear pattern, but showed several dots in each nucleus that co-localized with TRF1, consistent with the presence of RAD50 and MRE11 at telomeres (Fig. 2*a*). Similar co-localization was observed in dual IF with RAD50 and TRF2 (data not shown).

Co-localization of RAD50 and MRE11 with TRF1 and TRF2 was also observed in two human cell lines that maintain telomeric DNA using a telomerase-independent (ALT) pathway[23]. The ALT cell lines WI38VA13/2Ra and GM847 have extremely long and heterogenously sized telomeres, resulting in strong TRF1 and TRF2 signals[24] that co-localize with several proteins involved in DNA synthesis and repair as well as the PML protein[24] (Fig. 2*b*). Confirming the results with HeLa cells, the two ALT cell lines showed co-localization of RAD50 and MRE11 with TRF1 (Fig. 2*b*).

To assess whether the telomeric localization of RAD50 was mediated by TRF2, we characterized HeLa cells transiently expressing the dominant-negative allele of TRF2 (TRF2$^{\Delta B\Delta M}$), which inhibits the accumulation of the endogenous TRF2 on telomeres[3]. We used dual IF for RAD50 and TRF1 to determine the percentage of nuclei lacking RAD50 at telomeres in cells with

Table 1 • Effect of TRF2$^{\Delta B\Delta M}$ on the telomeric localization of RAD50

	Fraction of cells with reduced telomeric TRF2[a]	Fraction of nuclei without telomeric RAD50[b]	
		vector	TRF2$^{\Delta B\Delta M}$
Experiment 1	20%	3.6%	15%
Experiment 2	35%	4.0%	24%
Experiment 3	29%	3.6%, 5.7%	19%, 25%

[a]Expression of TRF2$^{\Delta B\Delta M}$ was induced by transfection of pTETNFlag-TRF2$^{\Delta B\Delta M}$ in conjunction with pUHD15-1 plasmid[3] in experiment 1; by using retroviral gene delivery (A. Smogorzewska and T.d.L., unpublished data) in experiment 2; or by transfection of pCDNA3-TRF2$^{\Delta B\Delta M}$ (J. Karlseder and T.d.L., unpublished data) in experiment 3. The immunofluorescence in experiment 3 was performed in duplicate and scored in a double-blind fashion. [b]Cells that contained three or more overlapping punctate signals in dual immunofluorescence with antibodies to TRF1 and RAD50 were scored positive for telomeric RAD50 staining.

normal TRF2 function and in cells expressing TRF2$^{\Delta B\Delta M}$ (Table 1). In control cells, the fraction of nuclei lacking telomeric RAD50 ranged from 3.6% to 5.7%. By contrast, in cultures that expressed TRF2$^{\Delta B\Delta M}$, 15–25% of the nuclei showed no co-localization of RAD50 and TRF1. This result suggested that the association of RAD50 with telomeres is (in part) dependent on TRF2 function. We have been unable to extend these data using the TRF2$^{\Delta B\Delta M}$-expressing cell lines T4 and T19 because the short telomeres in these cells result in severely reduced TRF1 signals.

Although these results suggest that TRF2 function is important for the localization of RAD50 to telomeres, there is no evidence for a direct interaction between the proteins in the MRE11 complex and TRF2. For instance, the MRE11 complex might bind to a TRF2-interacting partner such as RAP1. Human RAP1, unlike its yeast counterpart, lacks telomeric DNA binding activity and requires TRF2 to accumulate at telomeres[7], predicting that RAP1-interacting proteins would also depend on TRF2 for telomeric localization.

The localization of NBS1 in detergent-extracted nuclei was distinct from the RAD50 and MRE11 patterns. In this case, most interphase cells showed NBS1 throughout the nucleus, with strong signals over the nucleoli. A subset of the cells showed less nucleolar staining, however, and showed NBS1 at faint punctate sites that represented telomeric loci as revealed by the presence of TRF1 (Fig. 2*a*). The same two staining patterns were observed with a different anti-NBS1 antibody[25] (Mab 1E9B4, data not shown). These data indicate that the telomeric localization of NBS1 is confined to a minority of the cells, whereas RAD50 and MRE11 are detectable at telomeric sites in most interphase nuclei (Table 1). The variation in NBS1 localization was also observed in ALT cells lines, in which approximately 10% of the cells showed NBS1 at TRF1 sites (Fig. 2*b*, and data not shown).

To investigate whether the association of NBS1 with TRF2 and telomeres varies during the cell cycle, we arrested HeLa cells at G1/S using a thymidine/aphidicolin block. After release from the arrest, the cells progressed through S phase and G2/M synchronously as evidenced by FACS analysis (Fig. 3*a*). Cell extracts were characterized for the association of TRF2 with RAD50, MRE11 and NBS1. Although the steady-state concentrations of NBS1 and TRF2 did not change appreciably (Fig. 3*b*, and data not

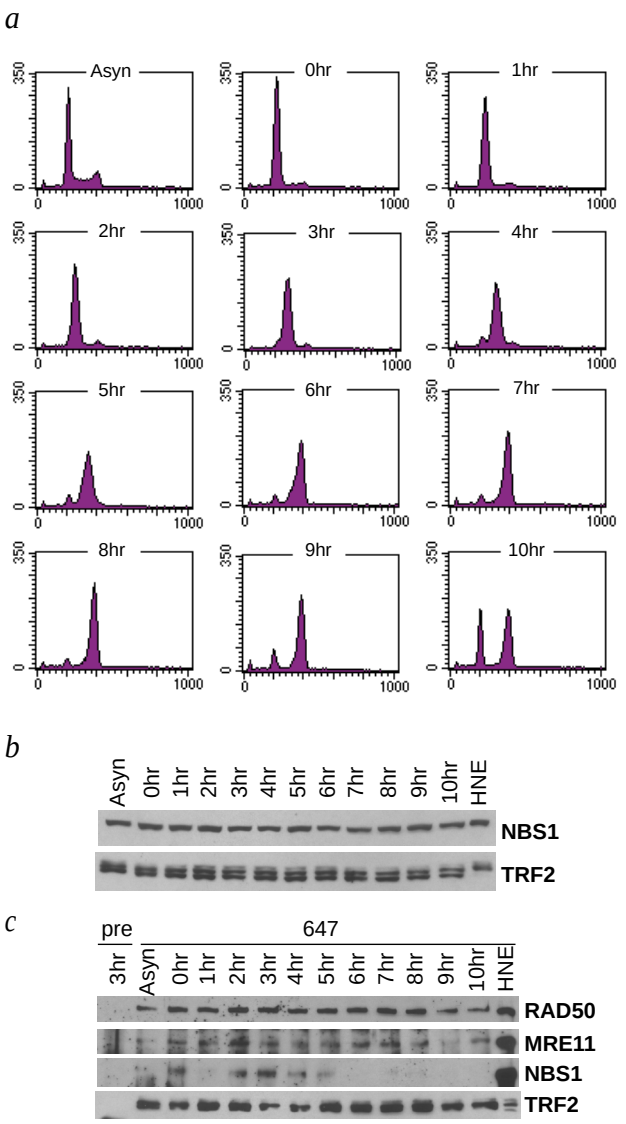

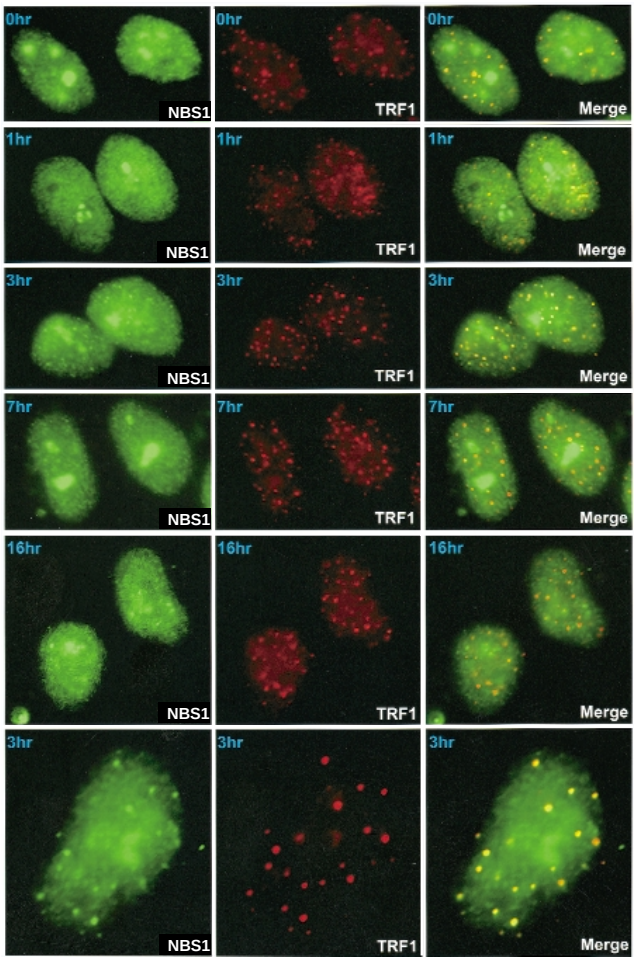

Fig. 3 Cell-cycle-regulated association of NBS1 with TRF2 and telomeres. ***a***, FACS analysis of synchronized HeLa cells. *y* axis, cell numbers; *x* axis, relative DNA content on the basis of staining with propidium iodide; 0–10 h, cells were released for 0-10 h from a thymidine/aphidicolin block; Asyn, asynchronous population. ***b***, Western-blot analysis of steady-state concentrations of NBS1 and TRF2. ***c***, Association of NBS1 with TRF2 in S phase. We carried out immunoprecipitations with either preimmune serum (pre) or anti-TRF2 (Ab#647) antibody and whole-cell extracts of HeLa cells collected at the indicated time points. We analysed TRF2 immunoprecipitates by western-blot analysis with anti-RAD50, anti-MRE11, anti-NBS1 and anti-TRF2. HNE, 20 μg of HeLa nuclear extract. ***d***, Cell-cycle-regulated localization of NBS1 at telomeres. We treated synchronized HeLa cells from the indicated time points as described in Fig. 2*a*. The fixed cells were dually stained with rabbit polyclonal anti-NBS1 antibody (FITC) and mouse anti-TRF1 antibody (TRITC).

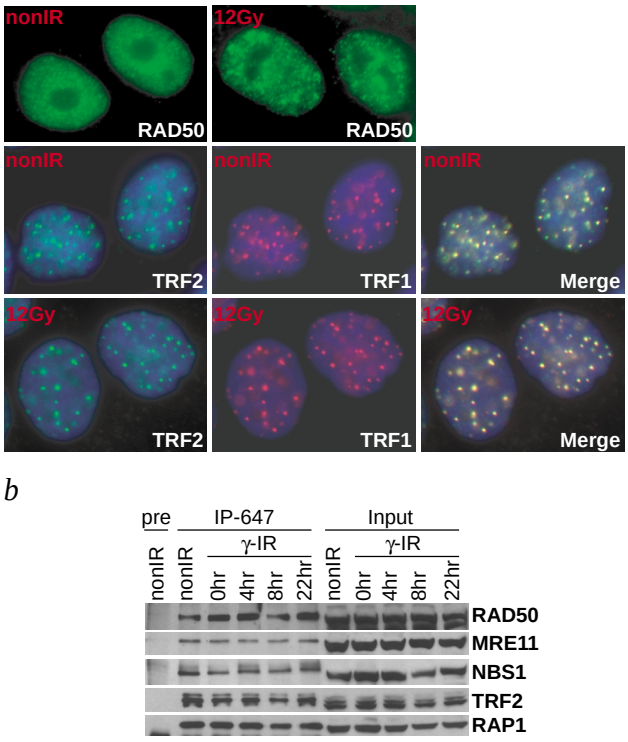

Fig. 4 γ-irradiation does not affect the telomeric localization of TRF2 or its interaction with the MRE11 complex. ***a***, Formation of RAD50 foci in γ-irradiated cells and persistence of TRF2 at telomeres. We γ-irradiated HeLa cells at a dose of 12 Gy. Non-irradiated cells were used as a control. The fixed cells were either immunostained with anti-RAD50 antibody alone (in green, FITC; top) or immunostained anti-TRF2 (#647; FITC) together with a mouse anti-TRF1 antibody (#3; TRITC). We stained DNA with DAPI. ***b***, γ-irradiation does not affect the association of RAD50/MRE11/NBS1 and RAP1 with TRF2. We carried out co-immunoprecipitations with anti-TRF2 antibody (#647) and cell extracts made from non-irradiated HeLa cells or cells collected at 0 h, 4 h, 8 h and 22 h post γ-irradiation. We loaded whole-cell extract from either non-irradiated or irradiated cells as input. We analysed the immunoprecipitates and inputs by western blot with anti-RAD50, anti-MRE11, anti-NBS1, anti-TRF2 and anti-RAP1 antibodies. We performed a control using pre-immune serum (pre) with non-irradiated cell extracts.

shown), there was a variation in the presence of NBS1 in the TRF2 complex (Fig. 3*c*). NBS1 was detected in the TRF2 complex in asynchronously growing cells and arrested cells, but disappeared from the complex within one hour after release from the block. As cells entered and progressed through S phase, NBS1 reappeared in the TRF2 complex and remained associated for several hours. At the end of S phase and in G2/M (7 h and later), NBS1 again disappeared from the TRF2 complex (Fig. 3*c*). In contrast to NBS1, the association of RAD50 and MRE11 with TRF2 was unaltered in G1, S and G2 (Fig. 3*c*).

The cell-cycle-dependent association of NBS1 with TRF2 was also reflected in its telomeric localization, which was obvious three hours after release from the thymidine/aphidicolin block when cells had entered S phase (Fig. 3*d*). By contrast, cells that had progressed through most of S phase (7 h; Fig. 3*d*) had little NBS1 at telomeres. NBS1 was also not observed at telomeres when most of the cells had entered G1 (16 h time point; Fig. 3*d*). A fraction of the cells arrested at G1/S showed NBS1 at telomeres, consistent with the co-immunoprecipitation data (Fig. 3*c*). These results suggest that the interaction of NBS1 with telomeres and TRF2 is mostly confined to S phase.

Because the MRE11 complex has been shown to migrate to sites of DNA damage in response to γ-irradiation[11], we wondered whether TRF2 participates in this re-localization. Although irradiated cells showed the expected accumulation of RAD50 radiation-induced foci (Fig. 4*a*), the localization of TRF2 remained unaltered, with most of the protein co-localizing with TRF1 on telomeres (Fig. 4*a*). Furthermore, TRF2 remained associated with the MRE11 complex for up to 22 hours after γ-irradiation (Fig. 4*b*). These data argue against a role for TRF2 in the response to double-strand breaks induced by γ-irradiation. Furthermore, it is unlikely that mammalian telomeres function as storage sites for the repair complexes, as has been proposed for yeast[26,27], because only a minor fraction of the MRE11 complex is located at telomeres and the association with TRF2 is not disrupted by irradiation.

Rather, the presence of the RAD50/MRE11/NBS1 complex at telomeres has implications both for the formation and function of the telomeric structure. Mammalian telomeres end in a large duplex loop[5] (t-loop). Closure of the t-loop is thought to involve the invasion of the 3′ telomeric overhang into the duplex telomeric repeat tract, creating a stable heteroduplex at the base of the loop. Formation of the t-loop thus resembles a DNA recombination event. The importance of the MRE11 complex for homologous recombination and non-homologous end-joining in yeast suggests that the complex may have a structural role in DNA recombination by stabilizing chromosomal interactions[13,28]. Similarly, the human MRE11 complex may facilitate t-loop formation by stabilizing the interaction between the invading terminus and the telomeric duplex in a manner that is analogous to its role in recombinational DNA repair. In this conception, t-loop formation is essentially a specialized intrachromosomal DNA-repair event mediated by the MRE11 and TRF2/RAP1 complexes. Retention of MRE11/RAD50 at the telomere may be required for the maintenance of t-loops through most of the cell cycle.

The transient recruitment of NBS1 in S phase suggests a role in telomere replication. Addition of NBS1 to RAD50 and MRE11 potentiates two *in vitro* enzymatic activities, a DNA helicase and an endonuclease that cleaves 3′ overhangs[29]. Recruitment of NBS1 to telomeric RAD50/MRE11 may thus regulate a helicase-mediated unpairing of the t-loop base and subsequently promote removal of the 3′ overhang by MRE11. This process would open the t-loop, perhaps facilitating progression of the DNA replication machinery to the end of the chromosome. Such a model also predicts that the MRE11 complex would be necessary for the release of the telomerase substrate, an accessible 3′ end, at chromosomal termini. Genetic experiments in yeast support such a role for the *S. cerevisiae* Mre11p complex[15,16], although t-loops have not been demonstrated in yeast. Resection of the 3′ overhang by the MRE11 complex may contribute to the high rate of telomere shortening observed in primary human cells[30].

Methods

Protein extracts. We prepared nuclear and whole cell extracts as described[3]. Briefly, we prepared nuclear extracts on ice by extraction of nuclei with 0.42 M KCl in buffer C (20 mM Hepes-KOH, pH 7.9, 25% glycerol, 0.1 mM EDTA, 5 mM $MgCl_2$, 1 mM dithiothreitol (DTT), aprotinin, leupeptin and pepstatin (each at 1μg/ml) and 0.5 mM phenylmethysulfonyl fluoride (PMSF)). We prepared whole-cell extracts by resuspending cell pellets in buffer C containing 0.42 M KCl and 0.2% Nonidet P-40. We then dialysed the extracts at 4 °C overnight against 100 mM KCl in buffer D (20 mM Hepes-KOH, pH 7.9, 20% glycerol, 0.2 mM EDTA, 0.2 mM EGTA, 1 mM DTT and 0.5 mM PMSF) and stored them at –80 °C. We determined protein concentrations using the Bradford assays (BioRad) with BSA as a standard.

Isolation of TRF2 complexes from HeLa nuclear extracts. For large scale IPs, we loaded nuclear extract from HeLa S3 cells (610 mg) on to a 5-ml heparin-sepharose column (Pharmacia Biotech) equilibrated in buffer D with 100

mM KCl and eluted with a 0.2–1 M KCl linear gradient. We pooled TRF2-containing fractions (from 0.5–1 M KCl) and dialysed against 100 mM KCl in buffer D. TRF2 immunoaffinity beads were prepared by cross-linking 68 μg of Ab#647 to 3.5 ml protein A beads (Pharmacia Biotech) using dimethylpimelimidate. We washed the cross-linked anti-TRF2 beads with glycine (0.1 M, pH 2.5), equilibrated with PBS, and incubated them with pooled TRF2-containing heparin column fractions in buffer D with 100 mM KCl and 0.1% Nonidet P-40. We washed beads containing TRF2 immunocomplex five times in buffer D containing 300 mM KCl and 0.2% Nonidet P-40, and we eluted bound proteins with glycine (0.1 M, pH 2.5). We precipitated the eluted proteins by 20% trichloracetic acid and 0.015% deoxycholate and fractionated on SDS–PAGE. We visualized proteins with Coomassie blue and bands corresponding to 150 kD, 70 kD (doublet) and 60 kD were excised for mass spectrometric analysis.

Mass spectrometry. We digested proteins in gel with trypsin (Roche Diagnostics) as described[31] and analysed the resulting peptides by nanoelectrospray tandem mass spectrometry[6] on a prototype quadrupole time-of-flight tandem mass spectrometer[32] (PE Sciex). We constructed peptide sequence tags[33] from the tandem mass spectra and searched against a non-redundant protein database (NRDB) maintained and updated regularly at the European BioInformatcis Institute (Hinxton) using the program PeptideSearch developed by M. Mann and colleagues at the EMBL. We verified peptide sequences of the retrieved proteins by matching the calculated fragment ion masses to signals observed in the respective tandem mass spectra.

Transfection and infection. We transfected HeLa cells transiently with either a Myc-tagged pCDNA3-TRF2$^{\Delta B\Delta M}$ or with pTetNFlag-TRF2$^{\Delta B\Delta M}$ in conjuction with pUHD15-1 plasmid[3]. As a control, we also carried out transfection with pCDNA3 vector or with the pTetNFlag vector in conjuction with pUHD15-1 plasmid[3]. We performed infection of HeLa cells with either retrovirus pLPCNMyc-TRF2$^{\Delta B\Delta M}$ or pLPCNMyc vector (A. Smogorzewska and T.d.L., unpublished data). We extracted cells with Triton X-100 and fixed them 24 h post-transfection or post-infection without drug selection.

Immunoblotting and immunoprecipitation. We raised TRF2 Ab#647 in a rabbit against purified [His]6-tagged full-length TRF2 expressed from baculovirus (bacTRF2). We raised mouse anti-TRF1 and mouse anti-TRF2 antisera in mice against full-length TRF1 and TRF2 expressed from baculovirus. Antiserum #765 to RAP1 has been described[7]. We affinity purified Ab#647 against bacTRF2 coupled to CNBr-activated agarose using standard procedures. We carried out immunoblotting as described[3] with HeLa nuclear extract (20 μg) or whole-cell extract (40 μg) fractionated on 8% SDS–PAGE and transferred to nictrocellulose. We performed immunoblots with monoclonal M2 anti-FLAG antibody (Sigma), mouse anti-TRF1 antibody or with rabbit antiserum against RAD50 (ref. 8), MRE11 (ref. 8), NBS1 (ref. 9), TRF1 (ref.20) (Ab#371), TRF2 (Ab#647) or RAP1 (Ab#765). We performed immunoprecipitation with whole cell extract (7 mg) and TRF2 preimmune serum, Ab#647 or M2 anti-FLAG antibody. Immunoprecipitates were fractionated on 8% SDS–PAGE, transferred to nitrocellulose and immunoblotted as described.

Immunofluorescence. We grew cells on coverslips, rinsed with PBS and then either fixed immediately or incubated in Triton X-100 buffer (0.5% Triton X-100, 20 mM Hepes-KOH, pH 7.9, 50 mM NaCl, 3 mM $MgCl_2$, 300 mM sucrose) at RT for 5 min before fixation. We carried out fixation in PBS-buffered 3% paraformaldehyde and 2% sucrose at RT for 10 min, followed by permeabilization in Triton X-100 buffer at RT for 10 min. For dual immunostaining, we blocked cells with 0.5% BSA (Sigma) and 0.2% gelatin (Sigma) in PBS and then incubated at RT for 2 h with either mouse anti-TRF1 (1:5,000) or mouse anti-TRF2 (1:1,500) in conjunction with affinity-purified rabbit antiserum (1:150) against RAD50, MRE11 and NBS1. Following incubation, we washed cells in PBS and incubated with fluorescein isothiocyanate (FITC)-conjugated donkey anti-rabbit and tetramethyl rhodamine isothiocyanate (TRITC)-conjugated donkey anti-mouse antibodies (1:100 dilution; Jackson Laboratories) at RT for 1 h. Cells were then washed and DNA was stained with 4, 6-diamidino-2-phenylindole (DAPI; 0.2 μg/ml). We recorded images on a Zeiss Axioplan microscope with either a Photometrics charge-coupled device camera or with a Hammamatsu C4742-95 camera, processed in either IP Lab or in Open Lab and merged in Adobe Photoshop.

Cell-cycle-analysis and γ-irradiation. We arrested exponentially growing HeLa1.2.11 cells in growth media with thymidine (2 mM) for 14 h followed by washing in PBS (three times) and release into fresh medium for 11 h. We then arrested cells a second time by addition of aphidicolin to a concentration of 1 μg/ml media followed by incubation for 14 h and then washed in PBS (three times) before release into fresh medium for 0–16 h. For FACS analysis, one million cells of asynchronous HeLa and synchronized HeLa cells that were released for 0–10 h were collected by trypsinization, and resuspended in PBS and 2 mM EDTA. We fixed cells in 70% ethanol, digested with RNase A (0.02 μg/μl), stained with 50 μg/ml propidium iodide, and analysed using a Becton-Dickinson FacsScan and CellQuest software. For γ-irradiation, we irradiated cells in a ^{137}Cs source at a dose of 12 Gy and collected them at the indicated time points.

Acknowledgements

We thank N. Heintz and W. Lee for HeLa nuclear extract; J. Karlseder for help with FACS analysis, pCDNA3-TRF2$^{\Delta B\Delta M}$ and comments on the manuscript; A. Smogorzewska for HeLa cells infected with TRF2$^{\Delta B\Delta M}$ retrovirus and comments on the manuscript; and B. Li, G. Celli, S. Smith and J. Ye for discussion. X.-D.Z. is supported by a Canadian MRC postdoctoral fellowship. B.K. was supported (in part) by a long-term post-doctoral fellowship from the EMBO. The laboratory of M.M. at the University of Southern Denmark is supported by a grant from the Danish National Research Foundation to the Center of Experimental BioInformatics (CEBI). J.H.J.P. is supported by NIH/NCI GM56888, GM59413 and the Milwaukee Foundation. This work was supported by a grant from the NIH (GM49046) to T.d.L.

Received 27 January; accepted 22 May 2000.

1. Broccoli, D., Smogorzewska, A., Chong, L. & de Lange, T. Human telomeres contain two distinct Myb-related proteins, TRF1 and TRF2. *Nature Genet.* **17**, 231–235 (1997).
2. Bilaud, T. *et al.* Telomeric localization of TRF2, a novel human telobox protein. *Nature Genet.* **17**, 236–239 (1997).
3. van Steensel, B., Smogorzewska, A. & de Lange, T. TRF2 protects human telomeres from end-to-end fusions. *Cell* **92**, 401–413 (1998).
4. Karlseder, J., Broccoli, D., Dai, Y., Hardy, S. & de Lange, T. p53- and ATM-dependent apoptosis induced by telomeres lacking TRF2. *Science* **283**, 1321–1325 (1999).
5. Griffith, J.D. *et al.* Mammalian telomeres end in a large duplex loop. *Cell* **97**, 503–514 (1999).
6. Wilm, M. *et al.* Femtomole sequencing of proteins from polyacrylamide gels by nano-electrospray mass spectrometry. *Nature* **379**, 466–469 (1996).
7. Li, B., Oestreich, S. & de Lange, T. Identification of human Rap1: implications for telomere evolution. *Cell* **101**, 471–483 (2000).
8. Dolganov, G.M. *et al.* Human Rad50 is physically associated with hMre11: identification of a conserved multiprotein complex implicated in recombinational DNA repair. *Mol. Cell. Biol.* **16**, 4832–4841 (1996).
9. Carney, J.P. *et al.* The hMre11/hRad50 protein complex and Nijmegen Breakage Syndrome: linkage of double-strand break repair to the cellular DNA damage response. *Cell* **93**, 477–486 (1998).
10. Haber, J.E. The many interfaces of Mre11. *Cell* **95**, 583–586 (1998).
11. Nelms, B.E., Maser, R.S., MacKay, J.F., Lagally, M.G. & Petrini, J.H.J. In situ visualization of DNA double-strand break repair in human fibroblasts. *Science* **280**, 590–592 (1998).
12. Lim, D.-S. *et al.* ATM phosphorylates p95/nbs1 in an S-phase checkpoint pathway. *Nature* **404**, 613–617 (2000).
13. Bressan, D.A., Baxter, B.K. & Petrini, J.H.J. The Mre11/Rad50/Xrs2 protein complex facilitates homologous recombination-based double strand break repair in *Saccharomyces cerevisiae*. *Mol. Cell. Biol.* **19**, 7681–7687 (1999).
14. Usui, T., Ohta, T., Oshiumi, J., Ogawa, T.H. & Ogawa, T. Complex formation and functional versatility of Mre11 of budding yeast in recombination. *Cell* **95**, 705–716 (1998).
15. Nugent, C. *et al.* Telomere maintenance is dependent on activities required for end repair of double-strand breaks. *Curr. Biol.* **8**, 657–660 (1998).
16. Boulton, S.J. & Jackson, S.P. Components of the Ku-dependent non-homologous end-joining pathway are involved in telomeric length maintenance and telomeric silencing. *EMBO J.* **17**, 1819–1828 (1998).
17. Le, S., Moore, J.K., Haber, J.E. & Greider, C.W. RAD50 and RAD51 define two pathways that collaborate to maintain telomeres in the absence of telomerase. *Genetics* **152**, 143–152 (1999).
18. Xiao, Y. & Weaver, D.T. Conditional gene targeted deletion by Cre recombinase demonstrates the requirement for the double-strand break repair Mre11 protein in murine embryonic stem cells. *Nucleic Acids Res.* **25**, 2985–2991 (1997).
19. Luo, G. *et al.* Disruption of mRad50 causes ES cell lethality, abnormal embryonic development and sensitivity to ionizing radiation. *Proc. Natl Acad. Sci. USA* **96**, 7376–7381 (1999).
20. van Steensel, B. & de Lange, T. Control of telomere length by the human telomeric protein TRF1. *Nature* **385**, 740–743 (1997).
21. Chong, L. *et al.* A human telomeric protein. *Science* **270**, 1663–1667 (1995).
22. Maser, R.S., Monsen, K.J., Nelms, B. & Petrini, J.H.J. hMre11 and hRad50 nuclear foci are induced during the normal cellular response to DNA double-strand breaks. *Mol. Cell. Biol.* **17**, 6087–6096 (1997).
23. Bryan, T.M., Englezou, A., Gupta, J., Bacchetti, S. & Reddel, R.R. Telomere elongation in immortal human cells without detectable telomerase activity. *EMBO J.* **14**, 4240–4248 (1995).
24. Yeager, T.R. *et al.* Telomerase-negative immortalized human cells contain a novel type of promyelocytic leukemia (PML) body. *Cancer Res.* **59**, 4175–4179 (1999).
25. Stewart, G. *et al.* The DNA double strand break repair gene hMre11, is mutated in individuals with a new ataxia telangiectasia like disorders (ATLD). *Cell* **99**, 577–587 (1999).
26. Martin, S.G., Laroche, T., Suka, N., Grunstein, M. & Gasser, S.M. Relocalization of telomeric Ku and Sir proteins in response to DNA strand breaks in yeast. *Cell* **97**, 621–633 (1999).
27. Mills, K.D., Sinclair, D.A. & Guarente, L. Mec1-dependent redistribution of the Sir3 silencing protein from telomeres to DNA double-strand breaks. *Cell* **97**, 609–620 (1999).
28. Moore, J.K. & Haber, J.E. Cell cycle and genetic requirements of two pathways of nonhomologous end-joining repair of double-strand breaks in Saccharomyces cerevisiae. *Mol. Cell. Biol.* **16**, 2164–2173 (1996).
29. Paull, T.T. & Gellert, M. Nbs1 potentiates ATP-driven DNA unwinding and endonuclease cleavage by the Mre11/Rad50 complex. *Genes Dev.* **13**, 1276–1288 (1999).
30. Harley, C.B. Telomeres and aging. in *Telomeres* (eds Blackburn, E.H. & Greider, C.W.) 247–265 (Cold Spring Harbor Press, Cold Spring Harbor, New York, 1995).
31. Shevchenko, A., Wilm, M., Vorm, O. & Mann, M. Mass spectrometric sequencing of proteins silver-stained polyacrylamide gels. *Anal. Chem.* **68**, 850–858 (1996).
32. Shevchenko, A. *et al.* Rapid 'de novo' peptide sequencing by a combination of nanoelectrospray, isotopic labeling and a quadrupole/time-of-flight mass spectrometer. *Rapid Commun. Mass Spectrom.* **11**, 1015–1024 (1997).
33. Mann, M. & Wilm, M. Error-tolerant identification of peptides in sequence databases by peptide sequence tags. *Anal. Chem.* 66, 4390–4399 (1994).